ELSEVIER

Earth and Planetary Science Letters 201 (2002) 525–540

EPSL

www.elsevier.com/locate/epsl

Fluid and chemical fluxes in and out of sediments hosting methane hydrate deposits on Hydrate Ridge, OR, I: Hydrological provinces

M.E. Torres [a,*], J. McManus [b,1], D.E. Hammond [c], M.A. de Angelis [d], K.U. Heeschen [e], S.L. Colbert [c], M.D. Tryon [f], K.M. Brown [f], E. Suess [e]

[a] *College of Oceanic and Atmospheric Sciences, 104 Ocean. Admin. Bld., Oregon State University, Corvallis, OR 97331-5503, USA*
[b] *Large Lakes Observatory, University of Minnesota, 10 University Dr, 109 RLB, Duluth, MN 58812, USA*
[c] *Department of Earth Sciences, University of Southern California, Los Angeles, CA 90089, USA*
[d] *Department of Oceanography, Humboldt State University, Arcata, CA 95521, USA*
[e] *GEOMAR, 1-3 Wischhofstrasse, D-24148 Kiel, Germany*
[f] *Scripps Institution of Oceanography, University of California, San Diego, 9500 Gilman Dr., La Jolla, CA 92093-0244, USA*

Received 1 August 2001; received in revised form 13 March 2002; accepted 20 May 2002

Abstract

Extensive deposits of methane hydrate characterize Hydrate Ridge in the Cascadia margin accretionary complex. The ridge has a northern peak at a depth of about 600 m, which is covered by extensive carbonate deposits, and an 800 m deep southern peak that is predominantly sediment covered. Samples collected with benthic instrumentation and from *Alvin* push cores reveal a complex hydrogeologic system where fluid and methane fluxes from the seafloor vary by several orders of magnitude at sites separated by distances of only a few meters. We identified three distinct active fluid regimes at Hydrate Ridge. The first province is represented by discrete sites of methane gas ebullition, where the bulk of the flow occurs through channels in which gas velocities reach 1 m s^{-1}. At the northern summit of the ridge the gas discharge appears to be driven by pressure changes on a deep gas reservoir, and it is released episodically at a rate of $\sim 6\times 10^4$ mol day^{-1} following tidal periodicity. Qualitative observations at the southern peak suggest that the gas discharge there is driven by more localized phenomena, possibly associated with destabilization of massive gas hydrate deposits at the seafloor. The second province is characterized by the presence of extensive bacterial mats that overlay sediments capped with methane hydrate crusts, both at the northern and southern summits. Here fluid typically flows out of the sediments at rates ranging from 30 to 100 cm yr^{-1}. The third province is represented by sites colonized by vesicomyid clams, where bottom seawater flows into the sediments for at least some fraction of the time. Away from the active gas release sites, fluid flows calculated from pore water models are in agreement with estimates using published flowmeter data and numerical model calculations. Methane fluxes out of

* Corresponding author.
E-mail address: mtorres@coas.oregonstate.edu (M.E. Torres).

[1] Present address: COAS, 104 Ocean. Admin. Bld., Oregon State University, Corvallis, OR 97331-5503, USA.

0012-821X/02/$ – see front matter © 2002 Elsevier Science B.V. All rights reserved.
PII: S0012-821X(02)00733-1

mat-covered sites range from 30 to 90 mmol m^{-2} day^{-1}, whereas at clam sites the methane flux is less than 1 mmol m^{-2} day^{-1}. © 2002 Elsevier Science B.V. All rights reserved.

Keywords: methane; hydrates; gas seeps; Cascadia subduction zone

1. Introduction

A seismic reflection survey on the Oregon continental margin indicates widespread presence of gas hydrates beneath the mid- and lower slope sections of this accretionary margin [1]. The bottom simulating reflector (BSR) is especially well developed beneath Hydrate Ridge [2], a 25 km long and 15 km wide ridge characterized by a northern peak at a depth of about 600 m, and a southern peak at approximately 800 m (Fig. 1). The northern summit represents a more mature stage in the evolution of these ridges [2], as evidenced by extensive carbonate pavement [3] and upward deflections of the BSR at a thrust fault [4,5]. In contrast, the southern region is less evolved, exhibiting only limited and localized carbonate build up and at most minor departures in BSR depth from that predicted by the seawater/gas hydrate phase boundary (A.M. Trehu, COAS, personal communication). Active fluid migration in the sediments underlying Hydrate Ridge was previously documented by seafloor camera tows and *Alvin* dives that revealed communities of vent-dependent organisms on its northern peak [3]. Gas discharge on the northern summit was first observed in 1996 [6]. Vigorous streams of methane bubbles emanating from the seafloor on the southern peak of Hydrate Ridge were recorded by video and acoustic data in 1999, on a region that was previously thought to be dominated by diffuse fluid flow [7].

Table 1
Site locations and cores used in this study

Site description	Station	Site	Latitude	Longitude	Depth m
Bacterial mats	A99-**5**-AD3421-CA, -CB	HRS	44°34.23′N	125°08.90′W	778
	A99-**8**-AD3422-BL				
	A99-**14**-AD3424-CA, -CB				
	A99-**14**-AD3424-BB				
	A99-**28A**-AD3428-BB				
	A99-**37**-AD3430-CA		44°34.20′N	125°08.82′W	768
	A99-**21**-AD3426-CA	HRN	44°40.03′N	125°06.01′W	600
	A99-**21**-AD3426-BB				
Clam fields	A99-**8**-AD3422-CA, -CB	HRS	44°34.22′N	125°08.90′W	778
	A99-**28B**-AD3428-BL				
	A99-**11**-AD3423-CB	HRN	44°40.03′N	125°06.01′W	600
	A99-**25**-AD3427-BB		44°40.20′N	125°05.88′W	593
Gas discharge	TFX98-**R455**-GS	HRN	44°40.17′N	125°05.89′W	587
	A99-**21**-AD3426-GS				
	A99-**25**-AD3427-BB				
Background sediment	A99-**28C**-AD3428-BL	HRS	44°34.25′N	125°08.98′W	791
Off-Hydrate Ridge	AD1907	First Ridge	44°40.44′N	125°17.63′W	2046
	AD2046		44°41.00′N	125°17.00′W	2100
	W8408-**4**	Abyssal plain	44°40.00′N	125°21.60′W	2860

Sites designated TFX98 were visited with *ROPOS* during 1998, those designated A99 were visited by *Alvin* in 1999; those designated AD1907 and AD2046 are *Alvin* dives on the First Ridge of the accretionary margin [10]. CA and CB designate push cores, GS indicates a gas sampling station, BB and BL indicate deployment of benthic barrel and benthic lander at the seafloor. HRS and HRN are Hydrate Ridge South and Hydrate Ridge North, respectively. Numbers in bold correspond to the station designation in Fig. 1.

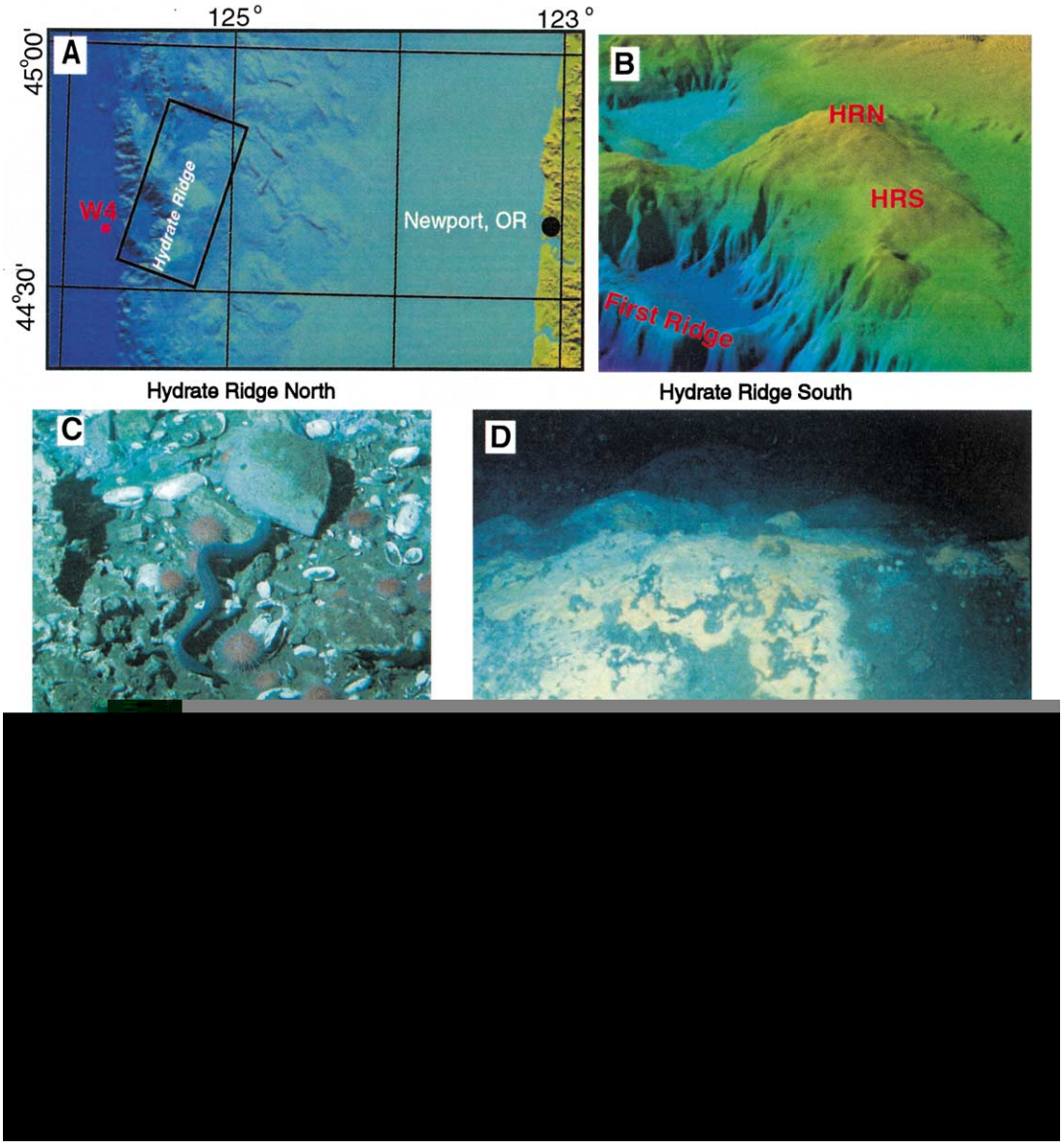

Fig. 1. A shows the location of Hydrate Ridge in the Cascadia accretionary margin (image from C. Goldfinger, Oregon State University, Corvallis, OR, USA). W4 designates the location of core W8408-4 in the Oregon abyssal plain. Box demarcates the location of Hydrate Ridge bathymetric image (oblique view) shown in B, which shows the location of the northern (HRN) and southern (HRS) summits of Hydrate Ridge surveyed during the 1998 and 1999 field seasons, and the location of the First Ridge, where cold seeps were discovered in 1987 [3]. The northern summit (HRN) is characterized by extensive carbonate deposits near and around the active venting sites, illustrated in C. The southern ridge (HRS) is predominantly sediment covered with sites of extensive bacterial mats overlying mounds several meters in diameter, as shown in D. Bathymetry and station locations on HRN (E) and HRS (F), detailed description of these sites is given in Table 1. Shading illustrates the areas characterized by active fluid seepage, where gas discharge, bacterial mats, clam colonies and gas hydrate deposits were observed.

and bacterial mats. When this crust was disturbed with an *Alvin* probe, large numbers of bubbles were released, leading to the conclusion that these crusts are formed, at least in part, from methane hydrate deposits. This observation was confirmed later by direct sampling of seafloor gas hydrates at this location with a TV-guided grab from the R/V *Sonne*, as well as by the observation of large blocks of methane hydrate floating at the sea surface [23]. It is conceivable that the hummocky topography may be generated by floating up of hydrate slabs at irregular intervals, with consequent release of the methane gas trapped beneath the gas hydrate crust to the bottom water [23].

Most bacterial mats overlay foci of upward advection of methane-rich fluids. To estimate the flow rates and the methane flux from these sites, we draw on data collected from benthic devices and pore water analysis. Fig. 4 summarizes the distribution of Ca^{2+}, and SO_4^{2-} for six cores collected at bacterial mat sites. In four of these cores, the curvature of the dissolved calcium profiles indicates upward fluid flow, whereas in two cores (21CB and 37CA) there is no change in calcium concentration with depth. The discrepancy in pore fluid distributions reflects the highly localized nature of the fluid pathway network on Hydrate Ridge.

At sites where calcium profiles are indicative of upward fluid flow, the advective rates can be estimated by applying a one-dimensional diffusion–advection–reaction model to the downcore Ca^{2+} concentration. Systematic variations in the concentration of pore water solutes have been shown to be reliable indicators of pore water flow (e.g. [24,25]). Here we used an approach parallel to that used by Han and Suess [26] to model the fluid flow regime of the first accretionary ridge, seaward of Hydrate Ridge (Fig. 1). This model assumes steady state, a constant diffusion coeffi-

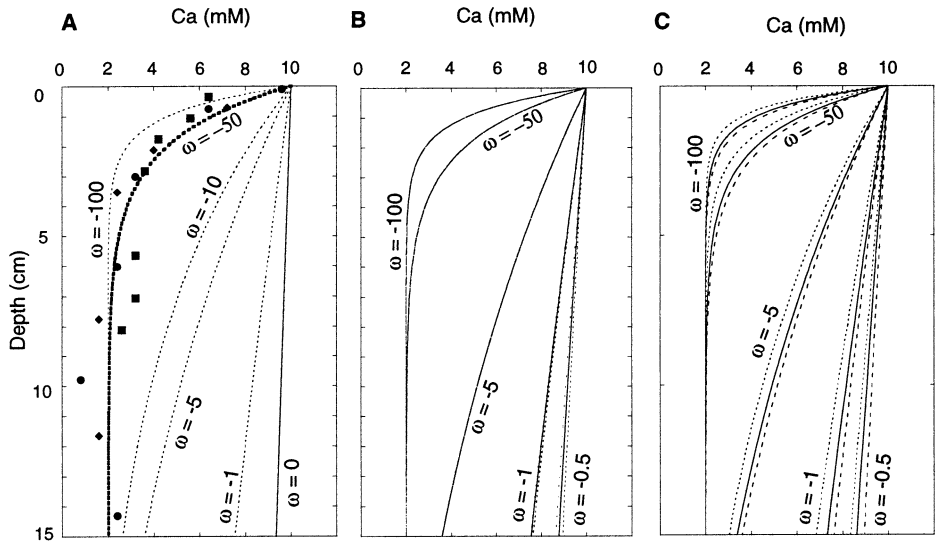

Fig. 5. Results of the one-dimensional model for estimating advective velocities (ω) based on dissolved calcium data. Up-flow is negative and it is given in cm yr^{-1}. A illustrates results of the model applied to a depth of 20 cm (dashed curves), indicating upward fluid velocities of 50–100 cm yr^{-1} for four cores (indicative of upward fluid flow) collected over bacterial mats on Hydrate Ridge. Symbols represent the different cores as shown in Fig. 4. Solid line represents the expected calcium distribution when there is no advective flow ($\omega = 0$), as calculated by Han and Suess [24] from calcium concentration data in core W8408-4 recovered from the Oregon abyssal plain. B and C illustrate the results of a sensitivity test of the model to changes in the apparent kinetic constant for calcium precipitation (k) and the diffusion coefficient for Ca^{2+} (D_s). The solid lines represent data for $k = 2\times10^{-4}$ yr^{-1} and $D_s = 2.85\times10^{-6}$ cm^2 s^{-1}. Effects of four-fold changes in the value of k are shown as dotted lines in B. These results demonstrate no significant changes in the modeled calcium distributions. The system is more sensitive to changes in diffusion coefficients, as shown by the dotted lines representing the expected Ca^{2+} profiles using values of D_s ranging from 2.5 to 3.3 cm^2 s^{-1} in C.

cient, constant porosity, and a first order reaction rate, and is given by:

$$D_s\frac{d^2C}{dz^2}-\omega\frac{dC}{dz}-kC=0 \quad (2)$$

where D_s is the diffusion coefficient for Ca^{2+}, C is the concentration of interstitial Ca^{2+}, z is the vertical depth (positive downward), ω is the advective rate of pore fluid (upwelling is negative), and k is the apparent kinetic constant for calcium precipitation. D_s is estimated to be 2.85×10^{-6} cm^2 s^{-1}, using the data of Li and Gregory [27] corrected for temperature (4 ± 1°C) and porosity effects [28]. We assume this value to be constant throughout the length of the cores ($z<20$ cm). Measured porosity in cores collected from this area shows a decrease of approximately 15% over the length of the cores, and changes in temperature over this depth are less than 0.2°C. Han and Suess [26] estimated the value for k to be 2×10^{-4} yr^{-1} using a core obtained at the abyssal plain (core W4, Fig. 1), where there is no fluid advection (i.e. $\omega=0$) and the calcium distribution is controlled exclusively by diffusion and reaction (Fig. 5A). We assume this value to represent the reaction rate on Hydrate Ridge. With these assumptions, the solution to Eq. 2 may be written as:

$$C(z)=C_1\exp(p_1z)+C_2\exp(p_2z) \quad (3)$$

, where $p=[\omega\pm(\omega^2+4kD_s)^{1/2}]/2D_s$, $C(z=0)=C_1+C_2$, and $C(z=h)=C_1\exp(p_1h)+C_2\exp(p_2h)$.

The values for $C(z=0)$ and $C(z=h)$ are the measured dissolved calcium concentration at the sediment water interface and the asymptotic calcium concentration at depth ($h=20$ cm), respectively. Using Eq. 3 we estimate the rate of fluid flow from four cores indicative of upward transport at bacterial sites, and obtain velocities that range from 50 to 100 cm yr^{-1} (Fig. 5A). To evaluate the possible errors in our calculation of advective flow rates, introduced by changes in diffusion coefficients and reaction rates at the Hydrate Ridge sites, we ran the model using different values for D_s and k. The results indicate that a fourfold range in the reaction rates has a negligible effect on the estimates of ω (Fig. 5B). The system is more sensitive to changes in diffusion coefficients; however, a change in D_s of 15% has no significant effect on our flow rate estimates, because of the speed of the pore water flow (Fig. 5C). This exercise provides confidence on our advective rate estimate of 50–100 cm yr^{-1}.

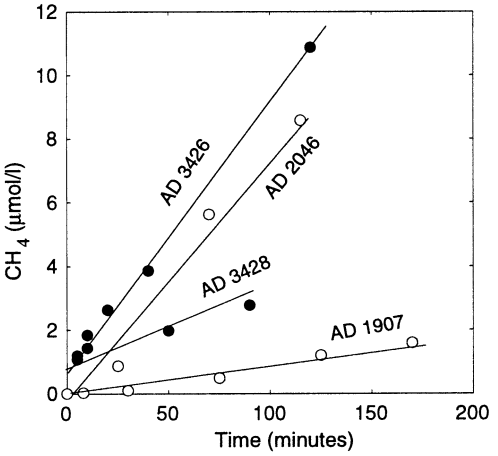

Fig. 6. Changes in methane concentration with time during deployment of the benthic barrel over bacterial mat fields on Hydrate Ridge (closed circles). The methane fluxes estimated from these data range from 30 to 90 mmol m^{-2} day^{-1}. Data obtained by deployment of this instrument over cold seeps on the First Ridge [10] are shown (open circles) for comparison. These data were used to estimate fluxes at the First Ridge ranging from 10 to 85 mmol m^{-2} day^{-1} [10].

Data collected using the benthic barrel provide additional confirmation of the fluid advection rates over bacterial mat sites, as well as allow us to estimate the methane flux at these locations. This instrument was deployed three times over bacterial mats overlying hydrated sediments during the *Alvin* cruise in 1999. During one of the deployments (AD3424), the surficial gas hydrate was highly disturbed, releasing the trapped methane gas. This release led to initial methane concentrations in the Niskin™ barrel samplers of 19 μM. The methane concentrations in all Niskin™ bottles during this deployment remained very high (>15 μM), and showed no systematic trend with time.

The changes in methane concentration during the other two deployments of the benthic barrel are shown in Fig. 6. This figure also includes

methane data collected with this instrument over seep sites on the seaward edge of the accretionary margin in 1987 [10,11] for comparison. The increase in methane concentration (μmol l^{-1}) with time is converted to total methane flux by multiplying it by the volume enclosed (180 l) and divided by the area covered by the barrel (0.26 m^2). Thus we calculate methane fluxes of 30 and 90 mmol m^{-2} day^{-1} for deployments during *Alvin* dives 3428 and 3426, respectively. In an attempt to estimate water flow from methane flux measurements we assume, as a first approximation, that methane behaves conservatively during the deployment period. This assumption is poor since the extensive bacterial mat coverage over these sites clearly indicates that these communities actively utilize methane. Indeed, dense aggregates of a structured bacterial archaea consortium have been identified in *Beggiatoa* mats collected from active seepage sites on Hydrate Ridge [29], which apparently mediate the anaerobic oxidation of methane. However, the rates of methane consumption reported for these sites [30] are less than 10 mmol m^{-2} day^{-1}, i.e. $<30\%$ of the estimated methane flux. Thus, although estimates of fluid flow from the methane fluxes are minimum values, we can obtain a first order estimate from:

$$\omega = J_{CH_4}/\phi C_{CH_4} \quad (4)$$

where J_{CH_4} is the methane flux, ϕ is the sediment porosity and C_{CH_4} is the concentration of methane in the discharging fluids. Because of the temperature and pressure changes that occur during core recovery, the in situ methane concentration in the seep sediments is difficult to constrain. However, since at these sites the barrel was deployed over sediments containing methane hydrate, we can determine the in situ methane concentration in the pore water using equilibrium values of dissolved methane in a methane/gas hydrate system at the temperature and pressure conditions of Hydrate Ridge [31,32]. Using this value (C_{CH_4} = 50 mM), we obtain estimates of flow rates that range from 30 to 100 cm yr^{-1}, which are consistent with our estimates based on the distribution of dissolved calcium in the pore water.

One 24 h deployment of the benthic lander over bacterial mats (8AD3422-BL) indicates variable flow rates at this location. The first 4 h period indicates downward flow, followed by 12 h in which upward flows exceeded 100 cm yr^{-1}. During the second half of this deployment, the radon flux was 128 ± 16 atoms m^{-2} s^{-1}, consistent with rapid upward advection of fluids. Apparently at bacterial mat sites there can be highly localized small-scale features with variable flow rates and directions.

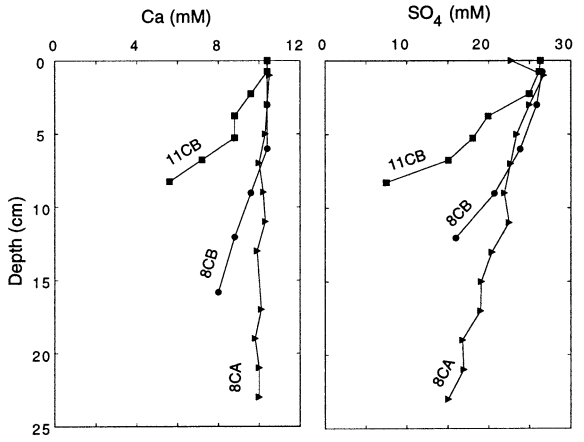

Fig. 7. Dissolved SO_4^{2-} and Ca^{2+} in pore fluids from cores collected from clam field sites. Cores 8CA and 8CB were collected about 8 m apart, within the same clam field. The site locations are given in Table 1 and are illustrated in Fig. 1.

3.3. Fluid flow at the clam sites

The third province on Hydrate Ridge is characterized by the presence of clam communities (Fig. 2C). The clam fields can extend for several tens of square meters of the seafloor, but the majority of these areas are covered by shell debris, particularly on the northern summit of the ridge. Patches of living clams can be found at the seafloor on both the northern and southern summits.

Deployment of chemical and aquatic transport (CAT) meters over clam fields on northern Hydrate Ridge in 1998 documents a pattern of predominantly downward flow at this location [8]. Not surprisingly, pore water profiles at sites colonized by vesicomyid clams (Fig. 7) are distinctly different from those observed on bacterial mat sediments (Fig. 4). The calcium profile from

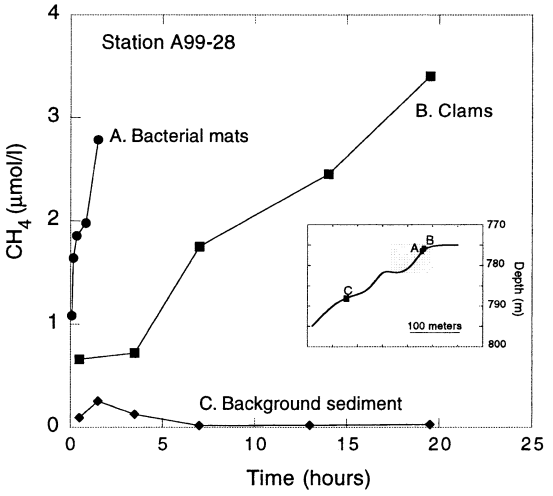

Fig. 8. Changes in dissolved methane concentration with time obtained by the simultaneous deployment of a benthic barrel and a benthic lander over a bacterial mat and a clam colony which were separated by less than 3 m (stations 28A and B). A second benthic lander was deployed during the same period of time over background sediments, 175 m away from the active sites, as shown in inset panel (station 28C). Site location is demarked in Fig. 1.

core 8CA is consistent with fluid flow into the sediments throughout the length sampled. A single barrel deployment over clam colonies during the 1999 cruise (AD3427) shows no measurable change in the methane content of the bottom water throughout the 2 h deployment, consistent with a system where the advective rate is very low or negative. A single 24 h deployment of a benthic lander over clam fields (28AD3428-BL, Table 1) did show a small increase in methane content over a 24 h period (Fig. 8). In addition to the methane discharge over the clam site, during this deployment we also measured the methane discharge over bacterial mats and background sediments in nearby sediments by simultaneously deploying three instruments. The data collected at all sites are shown in Fig. 8, and it further illustrates the heterogeneity of the methane discharge on Hydrate Ridge.

Using the benthic lander data, and the chamber configuration in this instrument (volume = 8 l; area = 700 cm^2), we estimate a methane flux out of sediments colonized by clams of 0.45 mmol m^{-2} day^{-1}. Methane concentration measurements on surface sediments from clam-populated sites yield values that range from 1 to 10 mM CH_4. A methane concentration of 1 mM in the upper 2 cm would result in a diffusive methane flux of 0.6 ± 0.4 mmol m^{-2} day^{-1}. Thus, most of the measured methane flux can be accounted for by diffusion. Similarly, the radon flux at this clam site was only 37 ± 9 atoms m^{-2} s^{-1}, and diffusion would supply 31 atoms m^{-2} s^{-1}. All these data are consistent with a negligible advective component.

The mechanisms driving the fluid flow at these sites are still controversial. Tryon et al. [8] explained the observed flow patterns as driven by the action of a 'gas pump' associated with episodic gas release, in a mechanism similar to that of a geyser. Wallman et al. [25] conclude that vent biota actively control the sediment water exchange and benthic fluxes at clam-colonized seep sites in the Aleutian margin. Alternatively, the observed profiles might reflect lateral fluid flow. Such lateral flow has been reported at cold seep regions in the Derugin Basin [33] and Monterey Bay [34] regions.

Table 2
Comparison of our estimates of fluid velocities at Hydrate Ridge with available data on rates of fluid flow at this location

Location		Technique	Advective rates cm yr^{-1}	Source
Hydrate Ridge	bacterial mats	pore water model	50–100	this study
		benthic barrel	30–100	this study
		CAT meters	10–250	[9]
Hydrate Ridge	clam sites	benthic landers	0	this study
		CAT meters	<6	[8]
Hydrate Ridge	thrust fault	benthic barrel/flowmeters	10^5	[11]
	thrust fault, ODP Site 892	hydraulic/thermal models	90–600	[35]

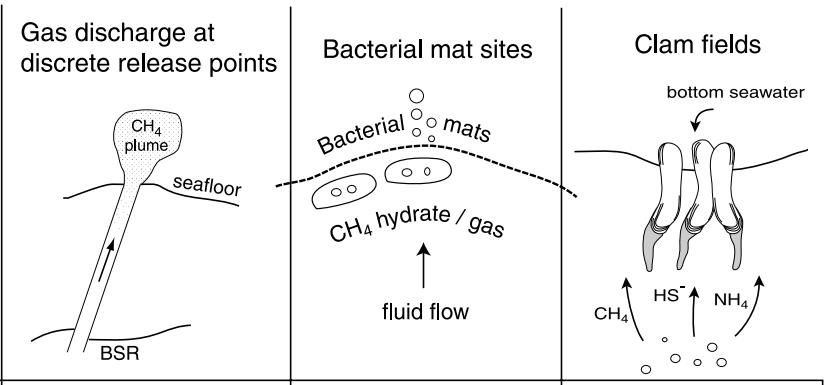

CH_4 conc.	methane content in the discharging gas: 99%	dissolved methane in equilibrium with methane hydrates = 50 mmol/l	methane content of the sediments 1 - 10 mmol/l
CH_4 flux mmol/m^2 day	app. 10^6	30 to 90	< 1
Fluid flux cm/yr	10^9 during maximum discharge periods	10 to 250	2 to -10
Flow transience	active gas flow lasts 2 to 6 hours; data suggests tidal control	hours to weeks	hours to weeks

Fig. 9. Summary representation of three provinces on Hydrate Ridge where fluid flow through the sediments modifies the composition of pore fluids and bottom water. The fluid flux data incorporate the results of this study and data from Tryon et al. [9], as shown in Table 2. The flow transience data at bacterial mats and clam sites are from Tryon et al. [9].

4. Discussion

The hydro-tectonic regime on Hydrate Ridge is clearly a highly dynamic system. Here we discuss the results of our field experiments in 1998 and 1999, in light of the overall knowledge gained by a wide range of investigations in this area, and compare the methane fluxes out of the Hydrate Ridge system with those obtained at other margins. A simplified cartoon of the three provinces described above, with estimated values for fluid velocities and methane fluxes are shown in Fig. 9. For completeness this figure also includes estimates of the periodicity of fluid flow reported by Tryon et al. [9].

4.1. Rates of fluid discharge

Our fluid flux estimates at sites colonized by clam colonies indicate flow rates below our detection capabilities. All of the CAT flowmeter data collected over clam sites on Hydrate Ridge by Tryon et al. [9] exhibit a low net rate of flow, generally < 10 cm yr^{-1}, often with complex variability and a predominance of bottom seawater flow into the sediment [9].

Fluid velocities at bacterial mat sites estimated in this study range from 20 to 100 cm yr^{-1} (Table 2). These values compare favorably with data collected at these sites with CAT meters, which range from 10 to 250 cm yr^{-1}, and average 85 cm yr^{-1} [9]. Indeed, Tryon et al. [9] collected flow rate data with their instrument at a site less than 1 m away from the location where the benthic barrel was deployed during AD3426; both instruments were placed within a single patch of bacterial mats. The CAT meter data (Meter 99-C) indicate a positive flow of 27–75 cm yr^{-1} during the period of time that the barrel was deployed at this site, consistent with our methane-derived flow rate estimate of 100 cm yr^{-1}. Numerical model calculations using hydraulic and thermal constraints yield values ranging from 90 to 600 cm yr^{-1} for fluid flow along a fracture zone on this margin [35]. On the other hand, Linke et al. [11] reported values as high as 10^5 cm yr^{-1} at this location.

Table 3
Comparison of dissolved methane fluxes at Hydrate Ridge with those from other sites of active seepage of fluids

Location		Release rates mmol m^{-2} day^{-1}	Source
Hydrate Ridge	bacterial mats	30–100	this study
Hydrate Ridge	clam fields	<1	this study
Hydrate Ridge	background sediments	non-detectable	this study
Hydrate Ridge	thrust fault (AD2283)	120	[11]
First Ridge	active seeps (AD1907, AD2046)	10–85	[10]
Peru margin	active seeps	52	M.E. Torres, unpublished data
San Clemente fault zone	active seeps	<1–300	[30]
Cape Lookout Bight, NC	diffusive flux	1–3	[37]

Such extremely high values are not consistent with our estimates or with the calculated flow velocities based on hydrogeologic models. Similar discrepancies between hydro-tectonic estimates and direct measurements during a 40 min deployment of a thermistor flowmeter were observed in the Aleutian margin [36]. The authors proposed that the discrepancies were due to localized effect of fluid pumping by vent biota [25]. Superimposed on the low hydro-tectonic flow, biota at these sites might generate an additional localized water circulation cell in which fluid moves at rates several orders of magnitude higher than that induced by geotectonic forcing [36].

4.2. Methane fluxes

Methane produced within the sediments of the Cascadia accretionary margin enters the water column via two distinct processes. In the dissolved form, advection of fluids and diffusion across concentration gradients results in methane fluxes to the bottom water over large areas of the prism. In the gas phase, methane is released at discrete sites. These sites appear to be restricted to the ridge summits and have not been observed on the first accretionary ridge.

Although present over large areas, the magnitude of the dissolved methane flux can vary by orders of magnitude across very small distances of the seafloor. To illustrate the spatial heterogeneity at a given location, we can compare data from three instruments that were deployed simultaneously along a transect that covered a bacterial mat, clam field and background sediments on Hydrate Ridge South during AD3428. A benthic

Table 4
Comparison of methane gas emissions at the seafloor

Location	Technique	Release rates mol day^{-1}	Area surveyed m^2	Source
Hydrate Ridge North	gas sampling at the vents	6×10^4	80	this study
Hydrate Ridge North	water column methane budgets	9×10^4	4.7×10^7	[22]
Hydrate Ridge South	water column methane budgets	6×10^4	3.7×10^7	[22]
Tommeliten field, North Sea, Norway sector	bubble discharge observations with a remotely operated vehicle	1×10^5	1.2×10^5	[38]
UK Block 15/25 (pockmark), North Sea	gas rate measurements	3×10^3	6.5×10^5	[38]
Cape Lookout Bight, NC	direct measurements of gas bubbles	1×10^4	1×10^6	[37]
Coal Point, Santa Barbara Channel	50 kHz sonar data	4×10^6	1.8×10^7	[39]
	probability distribution of active seeps worldwide	10^9–10^{10}	global estimate	[41]
Global	anomalies in $\delta^{13}C$ of dissolved inorganic carbon during the latest Paleocene	2×10^{10} over 10^4 yr	global estimate	[40]

barrel was positioned over a bacterial mat and a benthic lander was deployed over a clam colony less than 3 m away from the benthic barrel (stations 28A and B, Fig. 1F). A second benthic lander was deployed during the same period of time over sediments that showed no evidence of fluid discharge. This background station is 175 m away from the active sites occupied by the other two benthic instruments (station 28C, Fig. 1F). Changes in methane concentration with time measured during this experiment are plotted in Fig. 8. During this experiment the methane fluxes from the bacterial mats and clam field locations correspond to 30 and 0.45 mmol m^{-2} day^{-1}, respectively. There is no detectable methane flux out of the background sediments. Thus it is hard to extrapolate individual measurements over larger areas. Nevertheless, dissolved methane fluxes out of the sediments on Hydrate Ridge range from <1 to ~ 100 mmol m^{-2} day^{-1} (Table 3). The magnitude of the dissolved methane fluxes on Hydrate Ridge is similar to that reported for cold seeps located on the First Ridge of this accretionary prism (Fig. 6). Similar methane fluxes have also been observed at active seeps on the Peru margin (M.E. Torres, unpublished data) and the San Clemente fault zone [30]. For comparison, in the methane-saturated sediments of Cape Lookout Bight, the diffusive methane flux ranges from 1 to 3 mmol m^{-2} day^{-1} [37].

In addition to the dissolved methane flux driven by advective and diffusive transport through Hydrate Ridge sediments, methane is also discharged in the gas phase at discrete sites on the summit of the ridges. At the northern summit, we have estimated a methane gas discharge of approximately 6×10^4 mol day^{-1}. Based on extensive measurements of dissolved methane in the water column over Hydrate Ridge, Heeschen et al. [22] estimate an input of methane gas from the northern and southern peaks of approximately 9×10^4 and 6×10^4 mol day^{-1}, at each of these locations respectively (Table 4).

Seafloor and acoustic surveys [7] and water column data [22] from various topographic highs along the accretionary margin off the Oregon coast document further locales of active release of methane gas. If our methane discharge estimate of $\sim 6\times10^4$ mol day^{-1} at Hydrate Ridge North is comparable to the discharge rates at these other sites, then the methane discharge on the Cascadia margin might be similar in magnitude to that of previously reported areas of macro seepage worldwide [38,39] (Table 4). The gas discharged at Hydrate Ridge, though, pales in comparison to the proposed methane release by massive gas hydrate destabilization during the latest Paleocene thermal maximum, 55 million yr ago. Dickens et al. [40] propose a scenario in which methane is released from gas hydrates at a rate of 2×10^{10} mol day^{-1} over 10^4 yr to explain global anomalies in the $\delta^{13}C$ of the dissolved inorganic carbon (DIC) in seawater.

Acknowledgements

We appreciate the support at sea by the master and crew of R/V *Brown* and R/V *Atlantis*, and the dedication and expertise of the *ROPOS* and *Alvin* teams during the 1998 and 1999 cruises. We sincerely thank D. Colbert, C. Meredith, D. Hubbard and S. Kohlbry for their excellent assistance at sea and with post-cruise analyses. We are also grateful to C.A. Paulson for discussions on modeling the pore water transport. The manuscript greatly benefited from thorough reviews by G. Wheat and J. Whelan. The research was supported in the USA by WCNURP grant PF806880 and by NSF grants OCE-9731157, OCE-9730817, OCE-9815186, OCE-9811975 and OCE-9906944. In Germany this project was funded by the Federal Ministry of Science and Technology (Fkz 03G0143A and 03GO148A). ***[BOYLE]***

References

[1] M.E. McKay, G.F. Moore, G.R. Cochrane, J.C. Moore, L.D. Kulm, Landward vergence and oblique structural trends in the Oregon margin accretionary prism: Implications and effect on fluid flow, Earth Planet. Sci. Lett. 109 (1992) 477–491.

[2] A.M. Tréhu, M.E. Torres, G. Moore, E. Suess, G. Bohrmann, Temporal and spatial evolution of a gas hydrate-

bearing accretionary ridge on the Oregon continental margin, Geology 27 (1999) 939–942.
[3] L.D. Kulm, E. Suess, J.C. Moore, B. Carson, B.T. Lewis, S.D. Ritger, D.C. Kadko, T.M. Thornburg, R.W. Embley, W.D. Rugh, G.J. Massoth, M.G. Langseth, G.R. Cochrane, R.L. Scamman, Oregon Subduction Zone: Venting, fauna, and carbonates, Science 231 (1986) 561–566.
[4] G.K. Westbrook, B. Carson, R.J. Musgrave et al. (Eds.), Proceedings of the Ocean Drilling Program Scientific Results, vol. 146 (part 1), Ocean Drilling Program, College Station, TX, 1994.
[5] M. Kastner, K.A. Kvenvolden, M.J. Whiticar, A. Camerlenghi, T.D. Lorenson, Relation between pore fluid chemistry and gas hydrates associated with bottom-simulating reflectors at the Cascadia Margin, Sites 889 and 892, Proc. ODP Sci. Results 146 (part 1) (1995) 175–190.
[6] E. Suess, M.E. Torres, G. Bohrmann, R.W. Collier, J. Greinert, P. Linke, G. Rehder, A. Tréhu, K. Wallmann, G. Winckler, E. Zuleger, Gas hydrate destabilization: Enhanced dewatering, benthic material turnover and large methane plumes at the Cascadia convergent margin, Earth Planet. Sci. Lett. 170 (1999) 1–15.
[7] M.E. Torres, G. Bohrmann, K. Brown, M.A. de Angelis, D. Hammond, G. Klinkhammer, J. McManus, E. Suess, A. Tréhu, Geochemical observations on Hydrate Ridge, Cascadia Margin during R/V-ATLANTIS-cruise AT3-35b, COAS-Data Report 174, Oregon State University, Corvallis, OR, 1999.
[8] M.D. Tryon, K.M. Brown, M.E. Torres, A.M. Tréhu, J. McManus, R.W. Collier, Measurements of transience and flow cycling near episodic methane gas vents, Hydrate Ridge, Cascadia, Geology 27 (1999) 1075–1078.
[9] M.D. Tryon, K.M. Brown, M.E. Torres, Fluid and chemical flux at Hydrate Ridge: II. Observations and long-term records reveal insights into dynamic driving mechanisms, Earth Planet. Sci. Lett. 201 (2002) S0012-821X(02)00732-X.
[10] B. Carson, E. Suess, J.C. Strasser, Fluid flow and mass flux determinations at vent sites on the Cascadia margin accretionary prism, J. Geophys. Res. 95 (1990) 8891–8897.
[11] P. Linke, E. Suess, M. Torres, V. Martens, W.D. Rugh, W. Ziebis, L.D. Kulm, In situ measurement of fluid flow from cold seeps at active continental margins, Deep Sea Res. 41 (1994) 721–739.
[12] W.M. Berelson, D.E. Hammond, P. Giordani, Effects of sea-floor disturbance on benthic flux measurements in the continental margin off Southern California (Catalina Basin), G. Geol. (3a) 51 (2) (1989) 143–150.
[13] W.M. Berelson, D.E. Hammond, The calibration of a new free-vehicle benthic flux chamber for use in the deep sea, Deep Sea Res. 33 (1986) 1439–1454.
[14] S. Lammers, E. Suess, An improved head-space analysis method for methane in seawater, Mar. Chem. 47 (1994) 115.
[15] W.M. Berelson, D.E. Hammond, A. Eaton, A technique for the rapid extraction of radon-222 from water samples and a case study, in: B. Graves (Ed.), Radon, Radium and other Radioactivity in Groundwater, Lewis Publications, Chelsea, MI, 1987, pp. 271–281.
[16] E. Faber, W. Stahl, Analytic procedure and results of an isotope geochemical surface survey in an area of the British North Sea, in: J. Brooks (Ed.), Petroleum Geochemistry and Exploration in Europe, Blackwell Scientific Publications, Oxford, 1983, pp. 51–63.
[17] D.E. Hammond, S. Colbert, The use of Rn-222 to constrain characteristics of gas vents in the Cascadia Margin hydrate field, Geophys. Res. Lett., in preparation.
[18] R. K. Sinnott, Coulson and Richardson's Chemical Engineering vol. 6, Chemical Engineering Design, 2nd edn., Butterworth and Heinemann, Oxford, 1974, 966 pp.
[19] E.E. Davis, K. Becker, B. Carson, Long-term observations of pressure and temperature in Hole 892B, Cascadia accretionary prism, Proc. Ocean Drill. Prog. Sci. Results 146 (1995) 299–311.
[20] A. Schultz, J.R. Delaney, R.E. McDuff, On the partitioning of heat flux between diffuse and point source seafloor venting, J. Geophys. Res. 97 (1992) 12299–12314.
[21] J.R. Boles, J.F. Clark, I. Leifer, L. Washburn, Temporal variation in natural methane seep rate due to tides, Coal Oil Point area, California, J. Geophys. Res. 106 (2001) 27077–27086.
[22] K.U. Heeschen, R.W. Collier, M. deAngelis, P. Linke, G. Rehder, G. Klinkhammer, E. Suess, M. Whiticar, Methane sources, distribution, and fluxes at the cold vent locations of Hydrate Ridge, Cascadia Margin, Glob. Biogeochem. Cycles, submitted.
[23] E. Suess, M.E. Torres, G. Bohrmann, R.W. Collier, D. Rickert, C. Goldfinger, P. Linke, A. Heuser, H. Sahling, K. Heeschen, C. Jung, K. Nakamura, J. Greinert, O. Pfannkuche, A. Tréhu, G. Klinkhammer, M.J. Whiticar, A. Eisenhauer, B. Teichert, M. Elvert, Sea floor methane hydrates at Hydrate Ridge, Cascadia Margin, AGU Monogr. Natural Gas Hydrates: Occurrence, Distribution, and Detection Geophysical Monograph 124 (2001) 87–98.
[24] C.G. Wheat, R.E. McDuff, Mapping the fluid flow of the Mariana Mounds ridge flank hydrothermal system: Pore water chemical tracers, J. Geophys. Res. 100 (1995) 8115–8131.
[25] K. Wallman, P. Linke, E. Suess, G. Bohrmann, H. Sahling, M. Schlüter, A. Dählmannm, S. Lammers, J. Greinert, N. von Mirbach, Quantifying fluid flow, solute mixing, and biogeochemical turnover at cold vents of the eastern Aleutian subduction zone, Geochim. Cosmochim. Acta 61 (1997) 5209–5219.
[26] M.W. Han, E. Suess, Subduction induced pore fluid venting, the formation of authigenic carbonates along the Cascadia continental margin: Implications for the global Ca cycle, Palaeogeogr. Palaeoclimatol. Palaeoecol. 71 (1989) 97–118.
[27] Y-H. Li, S. Gregory, Diffusion of ions in sea water and in deep-sea sediments, Geochim. Cosmochim. Acta 38 (1974) 703–714.
[28] B.P. Boudreau, The diffusive tortuosity of fine-grained

unlithified sediments, Geochim. Cosmochim. Acta 60 (1996) 3139–3142.
[29] A. Boetius, K. Ravenschlag, C.J. Schubert, D. Rickert, F. Widdel, A. Gieseke, R. Amann, B.B. Jørgensen, U. Witte, O. Pfannkuche, A marine microbial consortium apparently mediating anaerobic oxidation of methane, Nature 407 (2000) 623.
[30] M.A. deAngelis, M.E. Torres, J. McManus, Methane oxidation within the seep sediments from the San Clemente escarpment, American Society of Limnology and Oceanography Summer meeting, Copenhagen, Denmark, June, 2000.
[31] S.L. Miller, The nature and occurrence of clathrate hydrates, in: I.R. Kaplan (Ed.), Natural Gases in Marine Sediments, Plenum, New York, 1974, pp. 151–177.
[32] Y.P. Handa, Effect of hydrostatic pressure and salinity on the stability of gas hydrates, J. Phys. Chem. 94 (1990) 2651–2657.
[33] E. Suess, G. Bohrmann, J. Greinert, A. Derkachev, R. Kulinich, A. Obzhirov, G. Winckler, Giant cold vents and barite mineralization in the Derugin Basin, AAPG Pacific Section Meeting, Monterey, CA, 1999.
[34] J.B. Martin, S. Day, C.G. Wheat, J. Plant, D.L. Orange, T.L. Lorenson, Sedimentary record of cold seeps, AAPG Pacific Section Meeting, Monterey, CA, 1999.
[35] D. Mann, N. Kukowski, Numerical modelling of focussed fluid flow in the Cascadia accretionary wedge, Geodynamics 27 (1999) 359–372.
[36] E. Suess, G. Bohrmann, R. von Huene, P. Linke, K. Wallmann, S. Lammers, H. Sahling, G. Winckler, R.A. Lutz, D. Orange, Fluid venting in the eastern Aleutian subduction zone, J. Geophys. Res. 103 (1998) 2597–2614.
[37] C.S. Martens, J. Val Klump, Biogeochemical cycling in an organic-rich coastal marine basin: I. Methane sediment–water exchange processes, Geochim. Cosmochim. Acta 44 (1980) 471–490.
[38] M. Hovland, A.G. Judd, The global production of methane from shallow submarine sources, Cont. Shelf Res. 12 (1992) 1231–1238.
[39] J.S. Hornafius, D. Quigley, B.P. Luyendyk, The world's most spectacular marine hydrocarbon seeps (Coal Oil Point, Santa Barbara Channel, California): Quantification of emissions, J. Geophys. Res. 104 (1999) 20703–20711.
[40] G.R. Dickens, M.J. Castillo, J.G.C. Walker, A blast of gas in the latest Paleocene: Simulating first-order effects of massive dissociation of oceanic methane hydrate, Geology 25 (1997) 259.
[41] M. Hovland, A.G. Judd, R.A. Burke Jr., The global production of methane from shallow submarine sediments, Chemosphere 26 (1993) 559–578.